

*Library Copy  
2A. A73 L 189*

UNCLASSIFIED  
~~CONFIDENTIAL~~

Copy 44  
RM SL57K2C

*218*

~~CONFIDENTIAL~~  
CLASSIFICATION CHANGED  
**NACA**  
~~CONFIDENTIAL~~

*(STAR)*  
By authority of *V. 9, No. 2* Date *6-30-71*  
*blm 9-17-71*

# RESEARCH MEMORANDUM

for the

Bureau of Aeronautics, Department of the Navy

RESULTS OF THE FLIGHT TEST OF A 0.13-SCALE ROCKET-BOOSTED  
MODEL OF THE McDONNELL F4H-1 AIRPLANE BETWEEN  
MACH NUMBERS OF 0.20 AND 1.90

REPORT NO. NACA AD 3115

By Earl C. Hastings, Jr., and Waldo L. Dickens

Langley Aeronautical Laboratory  
Langley Field, Va.

*UNCLASSIFIED*  
*Authority of NARA 115X1-101*  
*3/18*

~~CONFIDENTIAL~~  
~~CONFIDENTIAL~~

NOV 13 1957  
NOV 8 1957

CLASSIFIED DOCUMENT

This material contains information affecting the National Defense of the United States within the meaning of the espionage laws, Title 18, U.S.C., Secs. 793 and 794, the transmission or revelation of which in any manner to an unauthorized person is prohibited by law.

## NATIONAL ADVISORY COMMITTEE FOR AERONAUTICS

WASHINGTON

NOV 8 1957

~~CONFIDENTIAL~~

UNCLASSIFIED



NATIONAL ADVISORY COMMITTEE FOR AERONAUTICS

RESEARCH MEMORANDUM

for the

Bureau of Aeronautics, Department of the Navy

RESULTS OF THE FLIGHT TEST OF A 0.13-SCALE ROCKET-BOOSTED

**CLASSIFICATION CHANGED**

MODEL OF THE McDONNELL F4H-1 AIRPLANE BETWEEN

MACH NUMBERS OF 0.20 AND 1.90

**UNCLASSIFIED**

TED NO. NACA 3115

By authority of *CSTAR* *V-9 No. 2* Date *6-30-71*

By Earl C. Hastings, Jr., and Waldo L. Dickens

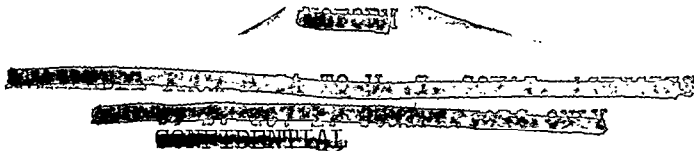
*blw 9-17-71*

SUMMARY

A flight test was conducted with a 0.13-scale rocket-boosted model of the McDonnell F4H-1 airplane configuration at transonic and supersonic speeds. The external drag coefficient varied from a value of 0.044 at a Mach number of 1.17 to 0.045 at a Mach number of 1.40 and then decreased to 0.041 at a Mach number of 1.90. At Mach numbers between 0.20 and 1.17, large pitching oscillations were experienced by the model; thus, it was not possible to compute the drag in this Mach number range. The limited oscillatory data available indicate the existence of a coupled longitudinal-lateral motion in the Mach number range from 0.20 to 1.17.

INTRODUCTION

An investigation is being conducted by the Langley Pilotless Aircraft Research Division at the request of the Bureau of Aeronautics, Department of the Navy, to determine the low-lift drag and longitudinal stability characteristics of the McDonnell F4H-1 airplane. This paper presents the results of a test conducted with a 0.13-scale rocket-boosted drag model of this airplane at the Langley Pilotless Aircraft Research Station at Wallops Island, Va.



**UNCLASSIFIED**

The purpose of the test reported herein was to determine the low-lift drag of this configuration at transonic and supersonic speeds. However, at Mach numbers less than 1.17 large pitching oscillations were experienced by the model; thus, it was not possible to compute drag below this Mach number from the limited amount of information available. The drag data, therefore, are presented at low-lift conditions between Mach numbers of 1.17 and 1.90 only. A qualitative discussion of the pitching oscillations below  $M = 1.17$  is included.

## SYMBOLS

The body-axes system shown in figure 1 indicates the positive directions of the forces, moments, and angles determined in this test.

A	cross-sectional area, sq ft
$a_{X/g}$ , $a_{Z/g}$	accelerometer readings along the X- and Z-axes, respectively
b	span, ft
$\bar{c}$	mean aerodynamic chord, ft
$C_D$	drag coefficient based on theoretical wing area
$C_L$	lift coefficient based on theoretical wing area
$C_X$	force coefficient along X body axis, $\frac{a_X}{g} \frac{W}{qS}$
$C_Z$	force coefficient along Z body axis, $\frac{a_Z}{g} \frac{W}{qS}$
g	acceleration due to gravity, ft/sec <sup>2</sup>
$i_t$	incidence of stabilator with respect to wing, deg
l	length of model fuselage, ft
m	mass of model, slugs
M	Mach number
$M_X$ , $M_Y$ , $M_Z$	rolling, pitching, and yawing moments about X-, Y-, and Z-axes, respectively
p	static pressure, lb/sq ft

$P_o$	rolling velocity, radian/sec
$P_t$	total pressure, lb/sq ft
$q$	dynamic pressure, lb/sq ft
$R$	Reynolds number based on wing mean aerodynamic chord
$S$	theoretical wing area, sq ft
$t$	time, sec
$V$	velocity, ft/sec
$W$	weight, lb
$w/w_\infty$	ratio of total mass flow through ducts to mass flow at free-stream conditions passing through an area equal to total inlet capture area
$x$	station measured from nose, ft
$X, Y, Z$	coordinate axes
$\alpha$	angle of attack of X-axis, deg
$\beta$	angle of sideslip, deg
$\gamma$	flight-path angle, deg, or ratio of specific heats
$\mu$	relative density factor, $\frac{m}{\rho S b}$
$\rho$	mass density of air, slugs/cu ft
$\phi$	roll angle, deg
$\psi$	yaw angle, deg
$\omega_\theta$	natural frequency of model in pitch, radian/sec
$\omega_\psi$	natural frequency of model in yaw, radian/sec
Subscripts:	
$b$	base
$e$	duct exit

i duct inlet (capture)  
W wing  
∞ free stream

## MODEL AND INSTRUMENTATION

### Model

The McDonnell F4H-1 airplane is a proposed two-place, all-weather interceptor. For this test a 0.13-scale rocket-boosted model of the airplane was supplied by the manufacturer and was instrumented at the Langley Laboratory in order to determine longitudinal trim and low lift drag data. A three-view drawing of the model is shown in figure 2, and figure 3 is a photograph of the model. Geometric and mass characteristics of the model are presented in table I and the normal cross-sectional-area distribution (which is based on values supplied by the manufacturer) is shown in figure 4.

Construction of the wing, vertical tail, and fuselage was primarily of internal steel members with castings and mahogany fairings forming the external contours. The wing had an aspect ratio of 2.82 and an incidence angle of  $1^\circ$  with respect to the longitudinal body axis. The aluminum-alloy stabilator was fixed at an angle of  $-3^\circ$  with respect to the wing. Both of the ducts were open to permit internal flow and were choked with sections at the rear selected to achieve the desired duct mass-flow ratio. Three total-pressure probes and six static-pressure orifices, located near the minimum section of one of the ducts, were used to determine average values of total and static pressure at the duct exit and six static-pressure orifices spaced around one of the duct bases were used to determine the average static pressure on the base of the duct. An enlarged drawing of the stationary adapter latch is also shown in figure 2. This latch was added by the Langley Laboratory to aid in the separation of the model from the booster and is not representative of any fixture on the full-scale airplane. The model was tested with the center of gravity located at 20.0 percent of the mean aerodynamic chord.

A 2.5-DS-59,000 (Nike) rocket motor was used to boost the model to the desired Mach number and, at burnout, the rocket motor separated from the model and allowed the model to coast through the test Mach number range. All the data presented in this paper were obtained during this coasting phase of the flight between Mach numbers of about 1.90 and 0.20. A photograph of the model-booster combination prior to launching is shown in figure 5.

## Instrumentation

The quantities necessary to determine the drag at low lift, longitudinal trim, and internal flow characteristics were transmitted to a ground receiving station by an internal telemeter system. The telemetered channels of information recorded were free-stream and duct-exit total pressures, accelerations along the X and Z body axes, angle of attack, and static pressures at the duct exit and on the base. Atmospheric conditions and winds aloft were determined from a rawinsonde released at time of firing. An NACA modified radar tracking unit was used to determine the position of the model in space and a CW Doppler velocimeter determined the velocity of the model. During the flight test the rolling velocity of the model was measured with a spinsonde by means of the polarized radio wave emanating from the telemeter antenna.

## REDUCTION OF DATA

The values of total lift coefficient and total drag coefficient were computed as

$$C_L = -C_Z \cos \alpha + C_X \sin \alpha$$

$$C_{D,tot} = -C_Z \sin \alpha - C_X \cos \alpha$$

and since the wing had  $1^\circ$  of positive incidence with respect to the X-axis

$$\alpha_w = \alpha + 1.00$$

In addition to values of  $C_{D,tot}$  from the measured telemeter data the CW Doppler radar values of velocity can be used to give an additional set of total-drag values. By differentiating this velocity with respect to time and adding the flight-path component of weight to obtain the drag deceleration, the total drag coefficient can be found by the following relationship:

$$C_{D,tot} = -\left(\frac{dV}{dt} + g \sin \gamma\right) \frac{W}{qSg}$$

where  $\gamma$  is the flight-path angle. A more complete discussion of this method of analysis can be found in reference 1.

The total base drag coefficient was computed from the expression

$$C_{D,b} = \frac{-2A_b(p_b - p_\infty)}{qS}$$

and the total internal drag coefficient was computed by the method of reference 2 expressed in terms of the equation

$$C_{D,int} = \frac{2A_e}{S} \left[ \frac{w}{w_\infty} \frac{A_i}{A_e} - \frac{p_e}{p_\infty} \left( \frac{M_e}{M_\infty} \right)^2 - \frac{p_e - p_\infty}{\gamma p_\infty M_\infty^2} \right]$$

where  $\gamma$  is the ratio of the specific heats. The external drag coefficient is defined as

$$C_{D,ext} = C_{D,tot} - C_{D,b} - C_{D,int}$$

ACCURACY

The following table presents what are believed to be reasonable values of total accuracy for the various parameters at several Mach numbers. Where possible, these values have been based on comparisons between several sources of data; and where a comparison was not possible, the values of accuracy have been estimated on the basis of instrument error.

Parameter	Total accuracy at -		
	M = 1.90	M = 1.17	M = 0.20
M . . . . .	0.010	0.010	0.10
$C_{D,tot}$ . . . . .	0.0015	0.0015	----
$\alpha$ , deg . . . . .	0.30	0.30	0.30
$C_{L,trim}$ . . . . .	0.02	0.03	----
$C_{D,b}$ . . . . .	0.0003	0.0003	----
$C_{D,int}$ . . . . .	0.0003	0.0003	----
$a_x/g$ . . . . .	-----	0.07	0.07
$a_z/g$ . . . . .	-----	0.80	0.80
$p_o$ , radian/sec . . . . .	3.0	3.0	----

## RESULTS AND DISCUSSION

## Test Conditions

Figures 6 to 10 present the test conditions necessary for evaluating the drag data. Shown in figure 6 is the variation of the parameters  $q$ ,  $V$ ,  $\mu$ ,  $R$ , and  $\rho$  with Mach number between 0.20 and 1.92. The relative density factor  $\mu$  is based on wing span and the Reynolds number  $R$  is based on the mean aerodynamic chord. The duct mass-flow ratio is presented in figure 7 where the data indicate that  $w/w_\infty$  increases with increasing Mach number. No values of  $w/w_\infty$  are presented for Mach numbers below  $M = 1.17$ . The variation of duct total-pressure recovery  $P_{t,e}/P_{t,\infty}$  is shown as a function of  $M$  in figure 8. These values should be considered qualitative since they were measured at the duct exit and therefore represent the loss in total pressure relative to the duct exit rather than to the engine face.

Longitudinal trim conditions of the model in terms of trim wing angle of attack  $\alpha_{w,trim}$  and trim lift coefficient  $C_{L,trim}$  are presented in figures 9 and 10, respectively. The changes in  $\alpha_{w,trim}$  and  $C_{L,trim}$  observed between about  $M = 1.17$  and  $M = 1.30$  were found by an examination of the time-history data to be changes in the steady-state conditions and are not associated with the beginning of the oscillatory motions of the model below  $M = 1.17$ . Figures 9 and 10 show that, between  $M = 1.17$  and  $M = 1.90$ ,  $\alpha_{w,trim}$  and  $C_{L,trim}$  are small, the maximum values being  $0.90^\circ$  and  $0.05$ , respectively.

## Drag

The variation of total drag coefficient  $C_{D,tot}$  with Mach number between  $M = 1.17$  and  $M = 1.90$  is shown in figure 11. These values are uncorrected for internal and base drag. Shown in this figure are values obtained from the telemetered accelerometer data and also from the CW Doppler velocimeter data. Agreement between the two sources of data is considered to be excellent throughout the Mach number range presented. No values of  $C_{D,tot}$  are presented at Mach numbers below  $M = 1.17$  since unexpected large oscillations at lower Mach numbers and the limited number of instruments installed in this model made it impossible to analyze the drag properly. A discussion of the oscillatory motions encountered at  $M < 1.17$  is presented subsequently.

Internal and base drag coefficients are presented in figure 12. The base drag coefficient  $C_{D,b}$  decreases from a value of  $0.0085$  at

$M = 1.17$  to  $0.0042$  at  $M = 1.90$ . Internal drag coefficient  $C_{D,int}$  increases with Mach number from a value of nearly zero at  $M = 1.17$  to  $0.0024$  at  $M = 1.90$ .

Figure 13 shows the values of  $C_{D,ext}$  which were determined by subtracting  $C_{D,b}$  and  $C_{D,int}$  of figure 12 from the faired curve of  $C_{D,tot}$  in figure 11. Estimates of the drag increment due to the adapter latch indicated a value of  $0.0003$  at  $M = 1.90$  and, since this increment is so small as to be well within the accuracy of the data, it has not been considered in correcting the total drag coefficient. At  $M = 1.17$ ,  $C_{D,ext}$  has a value of  $0.044$  and, at  $M = 1.40$ , increases slightly to a value of  $0.045$ . There is a gradual decrease in  $C_{D,ext}$  as the Mach number increases above  $M = 1.40$ , and at  $M = 1.90$ ,  $C_{D,ext} = 0.041$ .

Also shown in figure 13 are values of  $C_{D,ext}$  which were obtained from the data of reference 3 at Mach numbers of  $1.57$  and  $1.87$ . These values are the net external drag coefficients from the wind-tunnel tests of a  $1/20$ -scale model with the same stabilator setting and at the same lift coefficient as for the present test. The external inlet configurations of the two models were different but unpublished wind-tunnel data have shown that the effect of the inlet modifications on the external drag coefficient of this configuration is negligible. Although the large differences in Reynolds number conditions at which the two tests were conducted (about  $18 \times 10^6$  for the present test and about  $1.1 \times 10^6$  for the data of ref. 3) could influence the drag values, no attempt has been made in this paper to estimate this effect.

### Oscillatory Motions

At Mach numbers between  $0.20$  and  $1.17$ , the model experienced unexpected large pitching oscillations. Since the purpose of this investigation was to determine drag, the model was not sufficiently instrumented to allow a complete analysis of these motions. Figure 14 is a plot of  $a_x/g$ ,  $a_z/g$ ,  $\alpha$ , and  $M$  as functions of time between  $12.0$  seconds and  $30.0$  seconds (Mach numbers from  $1.18$  to  $0.19$ ). Since the pitching and yawing velocities and accelerations could not be accurately determined, the values of  $a_x/g$ ,  $a_z/g$ , and  $\alpha$  are uncorrected for model motions and should not be used for reduction of lift or drag coefficient.

Shown in figure 15 is the model rolling velocity  $p_0$  between  $M = 1.13$  and  $M = 1.90$  as determined from the spinsonde measurements. At Mach numbers less than  $1.13$  the rolling-velocity information available is believed to be unreliable and is not presented. The reason for

the high model rolling velocities between  $M = 1.13$  and about  $M = 1.40$  is not known, but rolling velocities of about 5 or 6 radians per second (as shown by the model between  $M = 1.40$  and 1.90) are not unusual in rocket-boosted model tests. In fact, estimates have indicated that the allowable tolerances in booster-fin alignment alone could impart a rolling velocity of 3.5 radians per second to the model at the separation Mach number ( $M = 1.96$ ). Asymmetries in the construction of the model could also contribute to the rolling velocity experienced in this Mach number range. Also plotted in figure 15 are the natural pitch and yaw frequencies  $\omega_\theta$  and  $\omega_\psi$ , respectively, of the model as estimated from information supplied by the manufacturer.

Although no extensive analysis of the oscillatory motions can be attempted, the data of figures 14 and 15 indicate that a coupled longitudinal-lateral motion existed at  $M = 1.17$  and probably continued to exist throughout the remainder of the flight-test Mach number range. The most significant indication of this result is that the Mach number at which the large pitch oscillations began corresponds very closely with that at which the model rolling velocity exceeds the estimated natural yawing frequency of the model. It was shown in reference 4 that coupling between the lateral and longitudinal modes of motion could result in unstable motions in the form of divergences if the airplane rolling velocity exceeded either of the uncoupled airplane natural frequencies in yaw or pitch. Figure 15 shows that in this test the large oscillations begin very close to the same Mach number at which the rolling velocity exceeds the estimated natural yaw frequency of the model. Another indication of coupling is that the motions recorded in pitch (as shown by the time histories of  $\alpha$  and  $a_z/g$  in fig. 14) are more characteristic of those associated with a coupled motion than of the sinusoidal oscillations generally associated with an uncoupled motion.

### CONCLUSIONS

From the results of the flight investigation of a 0.13-scale rocket-boosted model of the McDonnell F4H-1 airplane, the following conclusions are indicated:

1. At a Mach number of 1.17, the external drag coefficient had a value of 0.044 and, at a Mach number of 1.40, increased to a value of 0.045. This increase was followed by a gradual decrease in the external drag coefficient to a value of 0.041 at a Mach number of 1.90.

2. The model experienced a coupled longitudinal-lateral motion between Mach numbers of 0.20 and 1.17.

Langley Aeronautical Laboratory,  
National Advisory Committee for Aeronautics,  
Langley Field, Va., October 25, 1957.

#### REFERENCES

1. Wallskog, Harvey A., and Hart, Roger G.: Investigation of the Drag of Blunt-Nosed Bodies of Revolution in Free Flight at Mach Numbers From 0.6 to 2.3. NACA RM L53D14a, 1953.
2. Faget, Maxime A., Watson, Raymond S., and Bartlett, Walter A., Jr.: Free-Jet Tests of a 6.5-Inch-Diameter Ram-Jet Engine at Mach Numbers of 1.81 and 2.00. NACA RM L50L06, 1951.
3. Carmel, Melvin M., and Turner, Kenneth L.: Investigation of Drag and Static Longitudinal and Lateral Stability and Control Characteristics of 1/20-Scale Model of McDonnell F4H-1 Airplane at Mach Numbers of 1.57, 1.87, 2.16, and 2.53. Phase II Model - TED No. NACA AD 3115. NACA RM SL57A14, Bur. Aero., 1957.
4. Phillips, William H.: Effect of Steady Rolling on Longitudinal and Directional Stability. NACA TN 1627, 1948.

TABLE I.- DIMENSIONAL AND MASS CHARACTERISTICS OF THE 0.13-SCALE

## MODEL OF THE McDONNELL F4H-1 AIRPLANE

Wing:	
Area (theoretical), sq ft . . . . .	8.96
Area (including leading-edge extension), sq ft . . . . .	9.10
Span, ft . . . . .	4.99
Root chord (center line of model), ft . . . . .	3.05
Tip chord (theoretical), ft . . . . .	0.51
Mean aerodynamic chord, ft . . . . .	2.08
Incidence angle, deg . . . . .	1.00
Sweepback of leading edge, deg . . . . .	51.40
Sweepback of quarter-chord line, deg . . . . .	45.00
Sweepback of trailing edge, deg . . . . .	13.50
Taper ratio . . . . .	0.167
Aspect ratio . . . . .	2.82
Dihedral (inboard of base line 20.8), deg . . . . .	0.0
Dihedral (outboard of base line 20.8), deg . . . . .	12.00
Airfoil section at root . . . . .	NACA 0006.4-64 (modified)
Airfoil section at tip . . . . .	NACA 0003.0-64 (modified)
Stabilator:	
Total area, sq ft . . . . .	1.60
Span, ft . . . . .	2.30
Aspect ratio . . . . .	3.31
Taper ratio . . . . .	0.20
Sweepback of leading edge, deg . . . . .	42.45
Sweepback of quarter-chord line, deg . . . . .	35.50
Incidence angle with respect to wing, deg . . . . .	-3.00
Dihedral, deg . . . . .	-15.00
Root chord (center line of model) . . . . .	1.16
Tip chord, ft . . . . .	0.23
Mean aerodynamic chord, ft . . . . .	0.80
Airfoil section at root . . . . .	NACA 0003.7 - 64 (modified)
Airfoil section at tip . . . . .	NACA 0003.0 - 64 (modified)
Vertical tail:	
Area (as indicated in fig. 1), sq ft . . . . .	1.15
Taper ratio . . . . .	0.23
Aspect ratio . . . . .	0.60
Height (above fuselage and trailing-edge intersection), ft . . . . .	0.83
Root chord, ft . . . . .	2.24
Tip chord, ft . . . . .	0.51
Mean aerodynamic chord, ft . . . . .	1.56
Sweepback of leading edge, deg . . . . .	65.00
Ducts:	
Inlet capture area per side, sq in. . . . .	11.62
Exit area per side, sq in. . . . .	7.50
Base area per side, sq in. . . . .	11.80
Fuselage and nacelles:	
Length, ft . . . . .	7.28
Width (maximum), ft . . . . .	1.16
Depth (maximum), ft . . . . .	0.82
Maximum frontal area (fuselage alone), sq ft . . . . .	0.43
Maximum frontal area (including nacelles), sq ft . . . . .	0.78
Weight and balance:	
Weight, lb . . . . .	436.0
Wing loading, lb/sq ft . . . . .	48.7
Center of gravity, percent $\bar{c}$ . . . . .	20.0
Moment of inertia in pitch, slug-ft <sup>2</sup> . . . . .	36.66

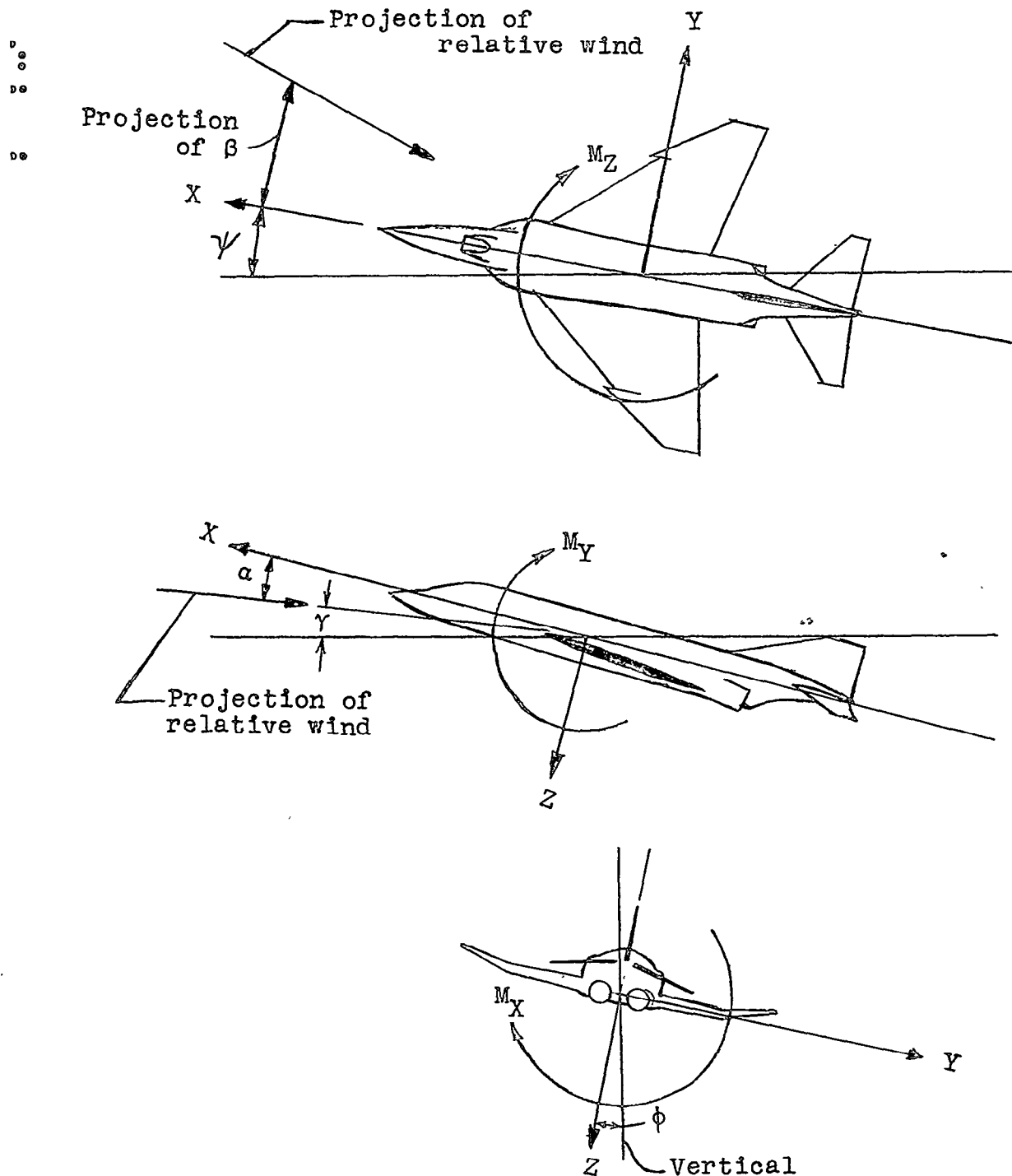


Figure 1.- Sketch showing the body axes system. Each view presents a plane of the axis system as viewed along the third axis. Arrows indicate positive directions of forces, moments, and angles.

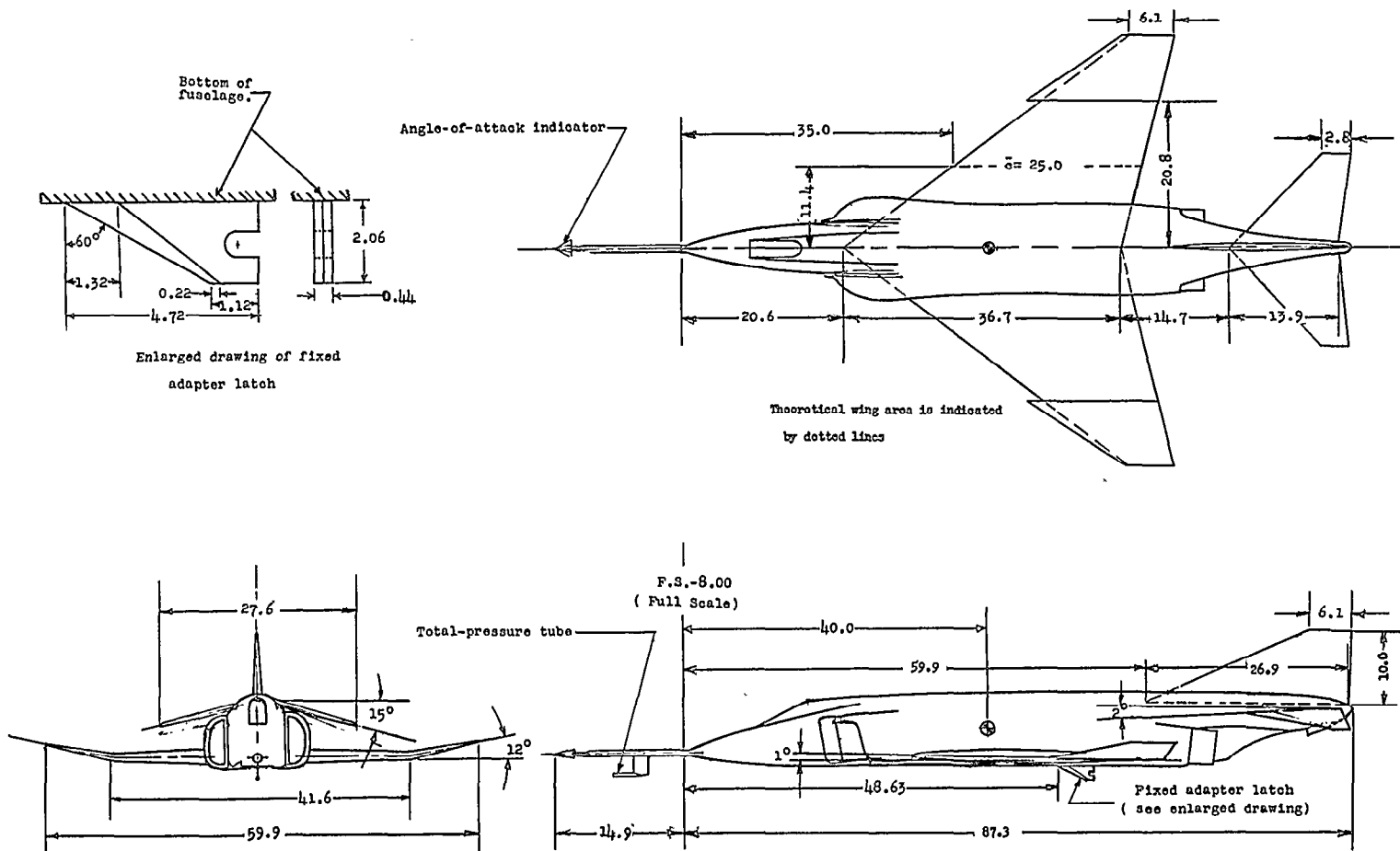


Figure 2.- Three-view drawing of the model. All dimensions are in inches.

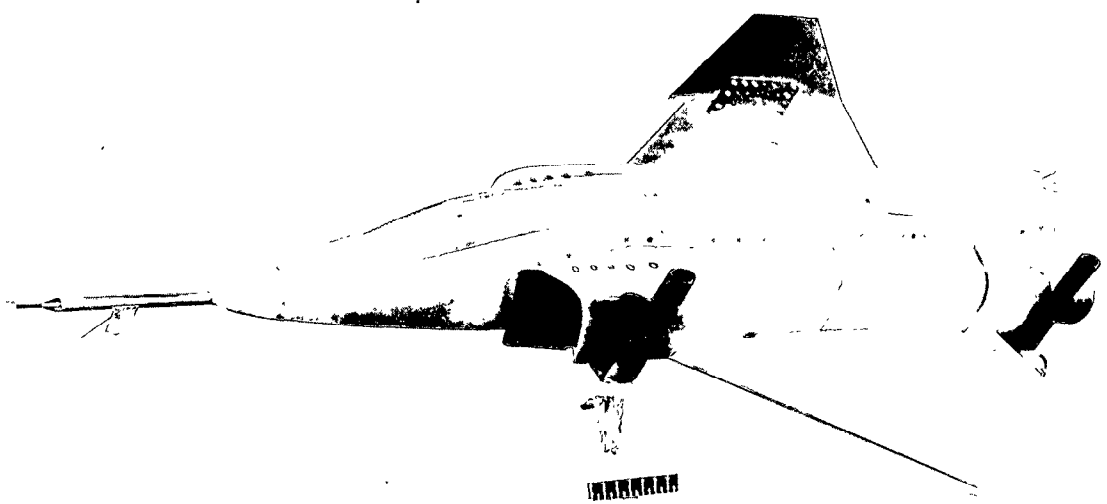


Figure 3.- Photograph of model.

L-57-2197

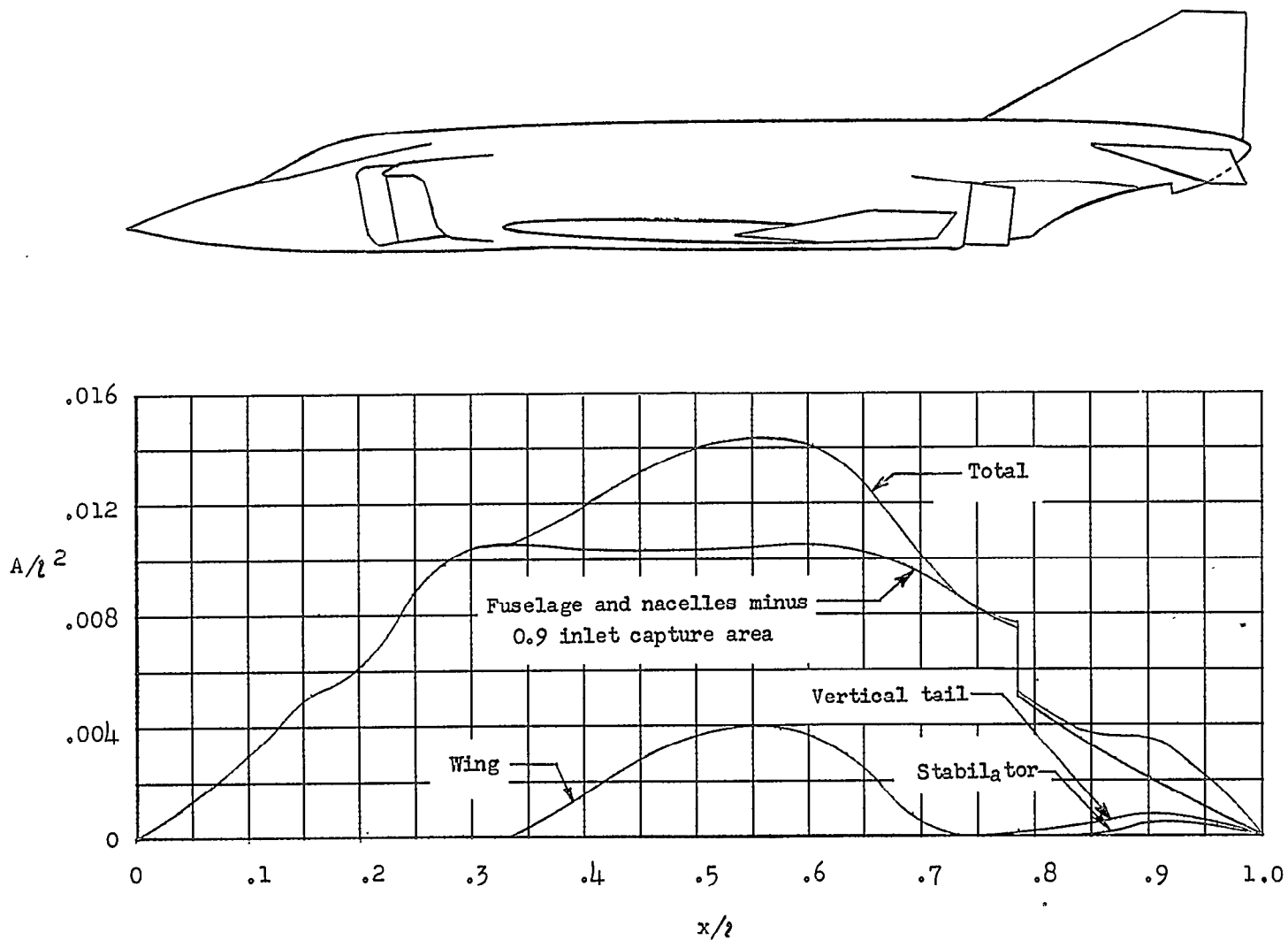
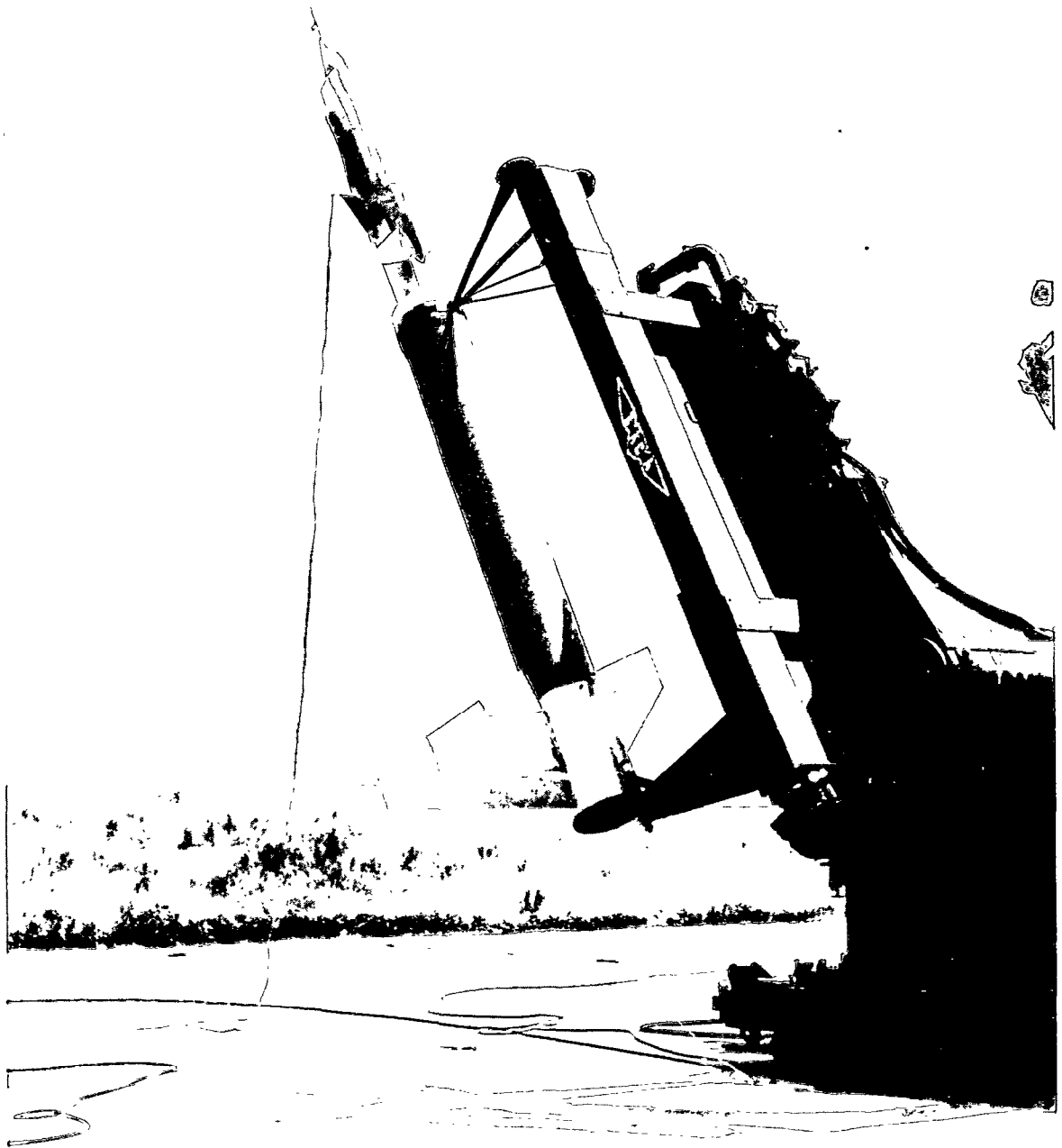


Figure 4.- Normal cross-sectional-area distribution of model.

DO  
O  
DO  
O  
DO  
O



L 57-2809  
Figure 5.- Photograph of the model-booster combination on the launcher.

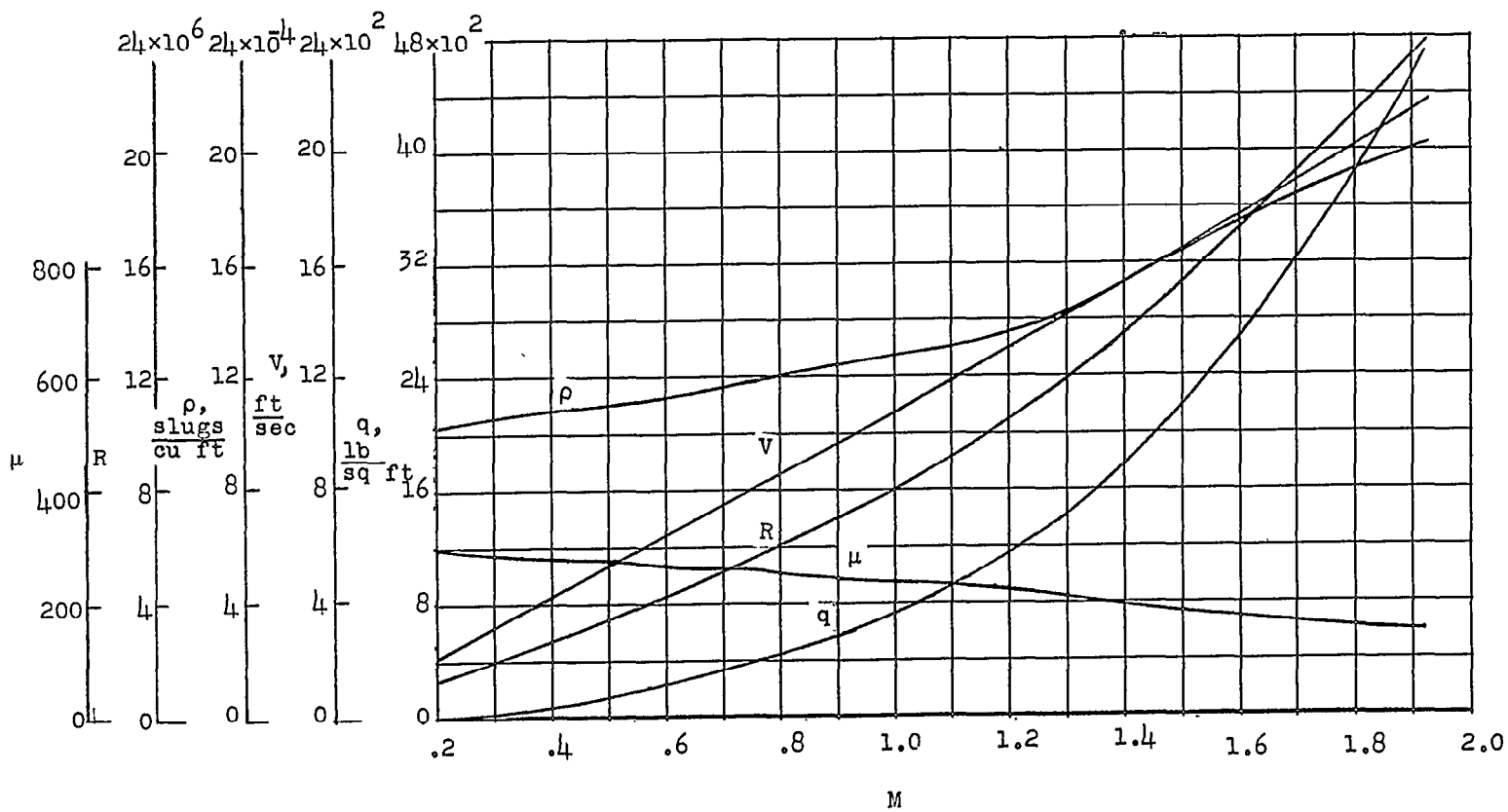


Figure 6.- Variation of velocity, dynamic pressure, air density, relative-density factor, and Reynolds number with Mach number.

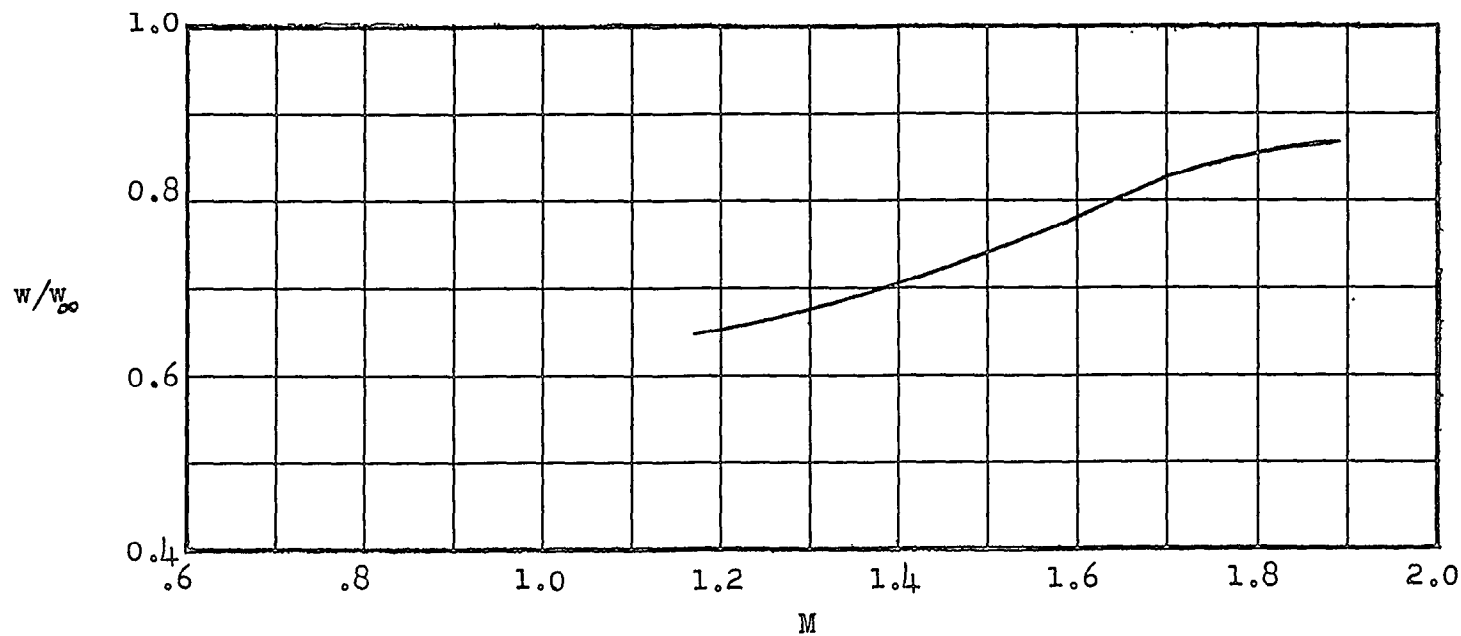


Figure 7.- Mass-flow ratio as a function of Mach number.

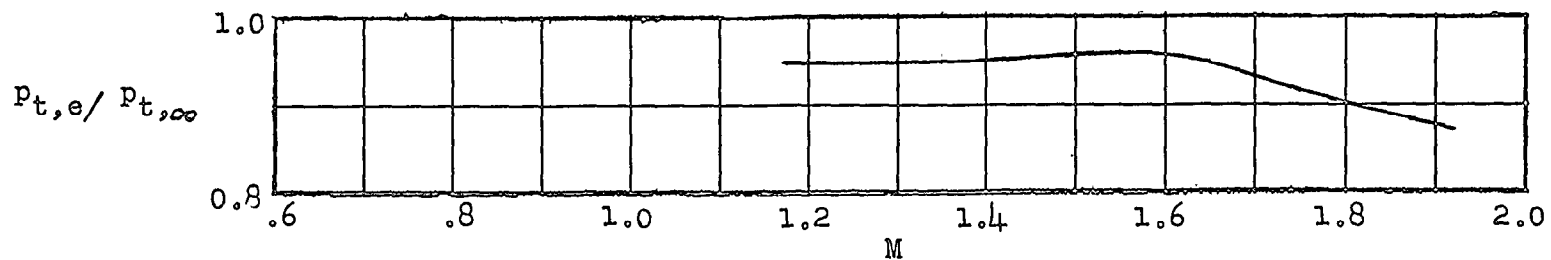


Figure 8.- Total-pressure recovery as a function of Mach number.

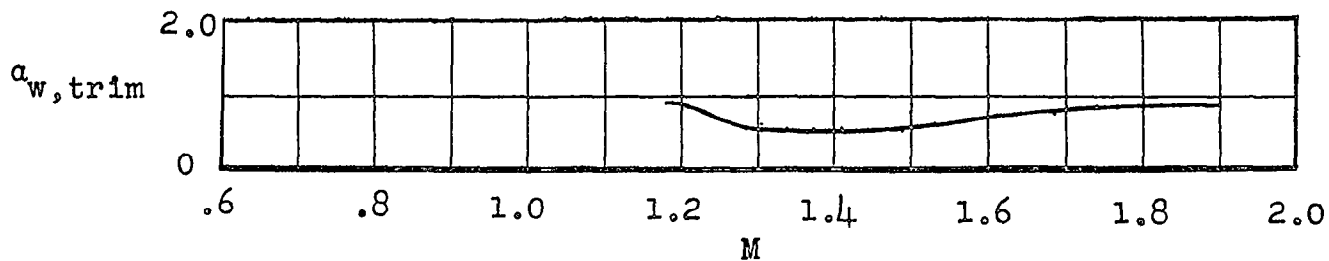
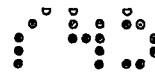


Figure 9.- Trim wing angle of attack. Center of gravity,  $0.20\bar{c}$ ;  $i_t = -3^\circ$ .

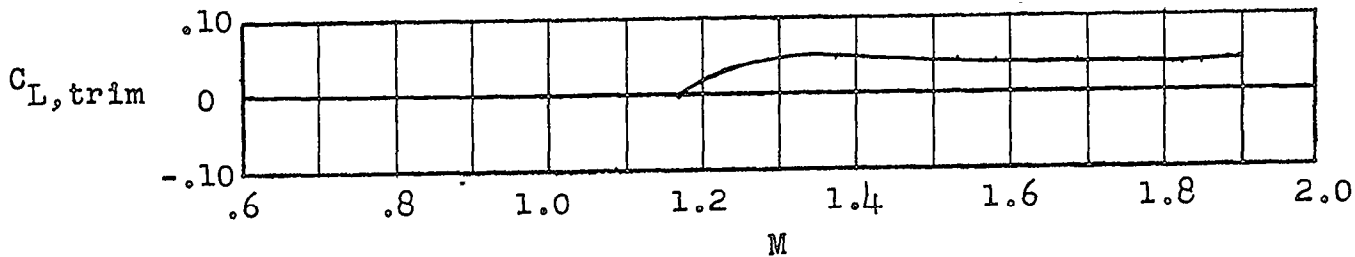


Figure 10.- Trim lift coefficient. Center of gravity,  $0.20\bar{c}$ ;  $i_t = -3^\circ$ .

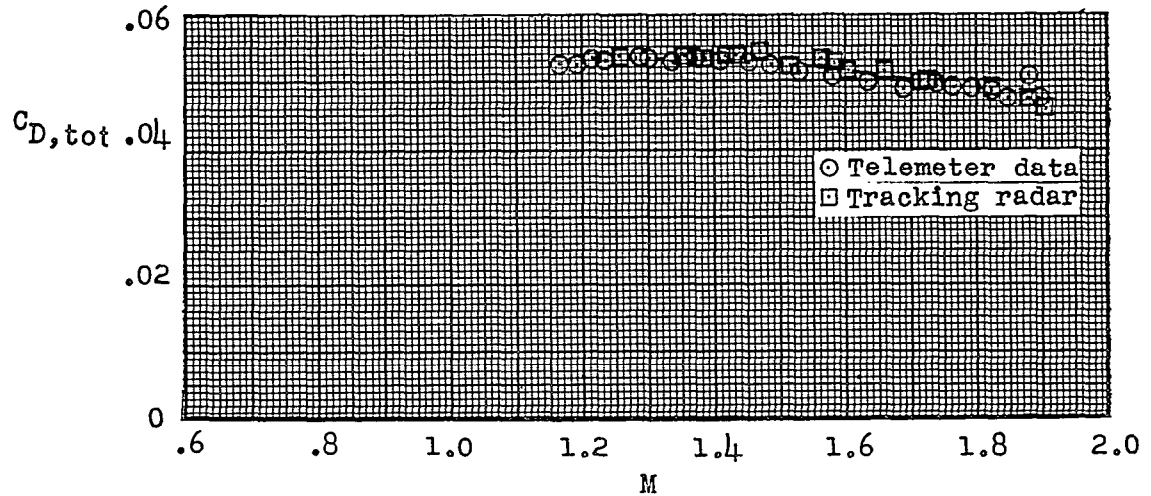
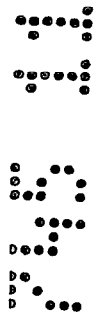


Figure 11.- Total drag coefficient.

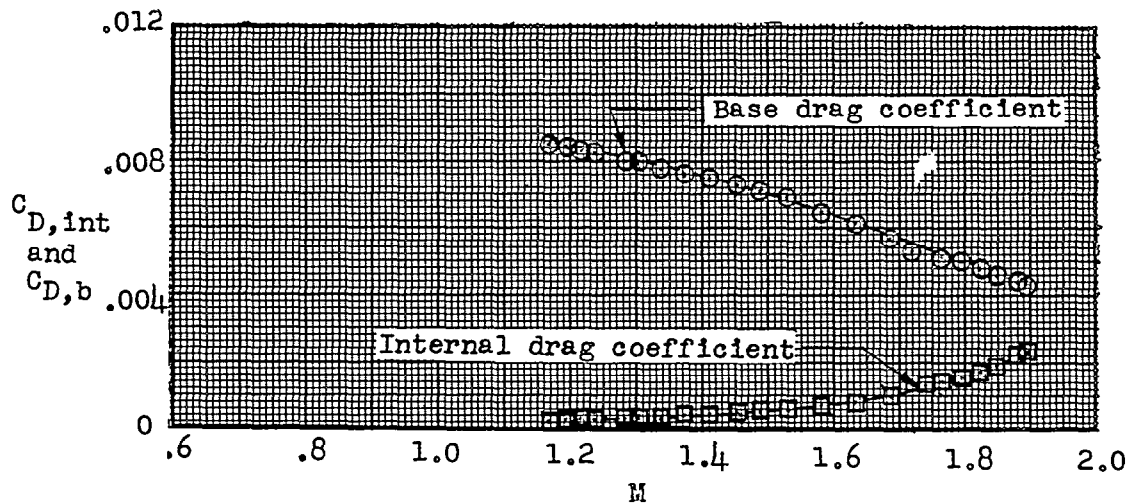


Figure 12.- Internal and base drag coefficients.

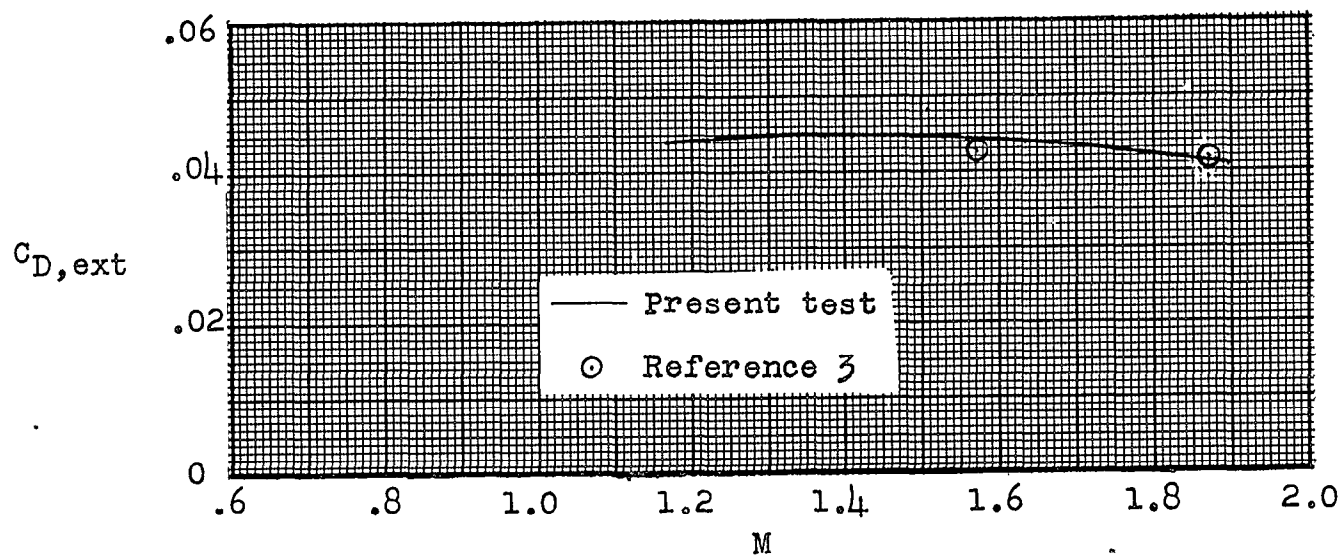
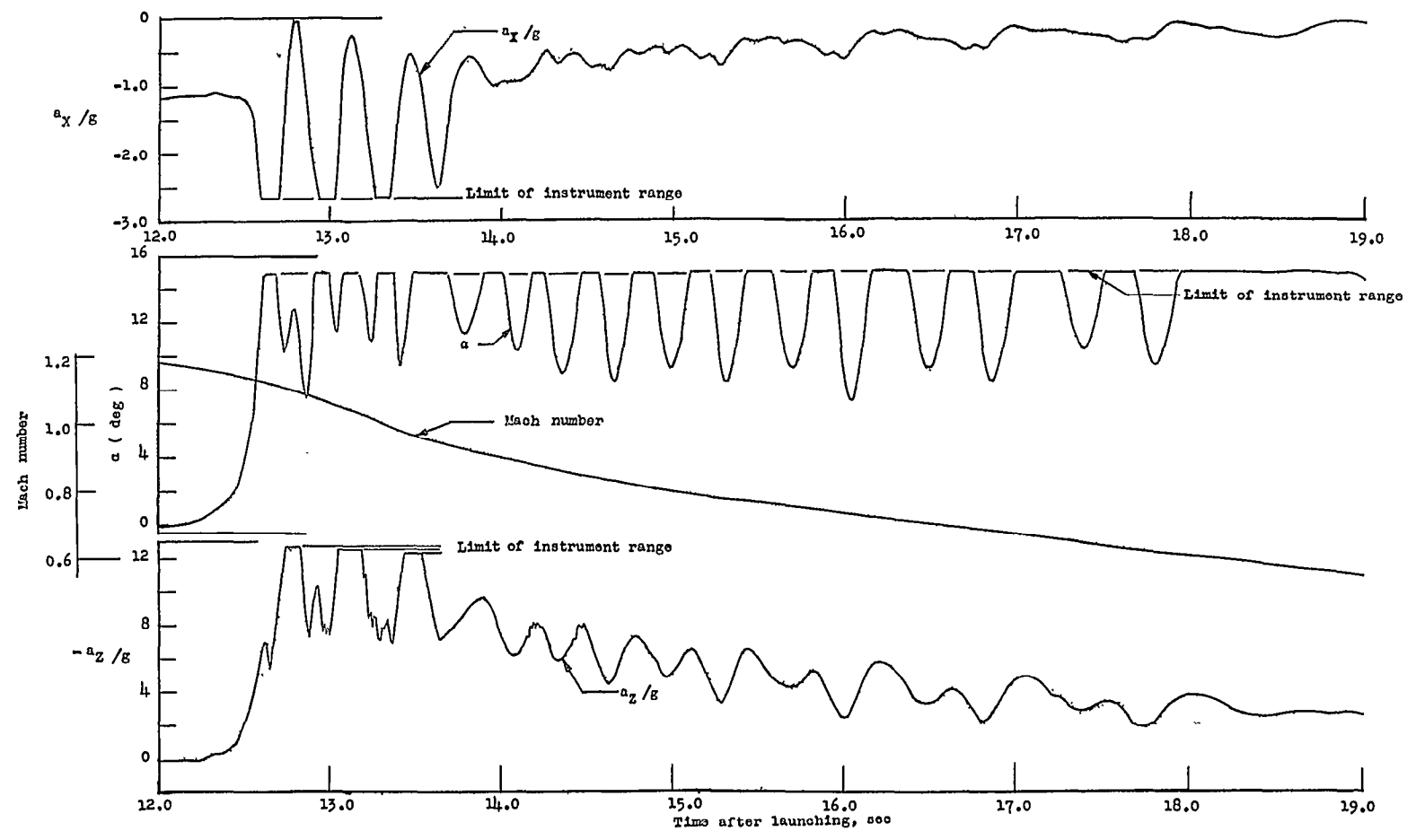
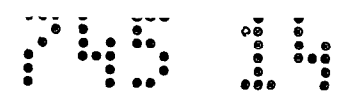
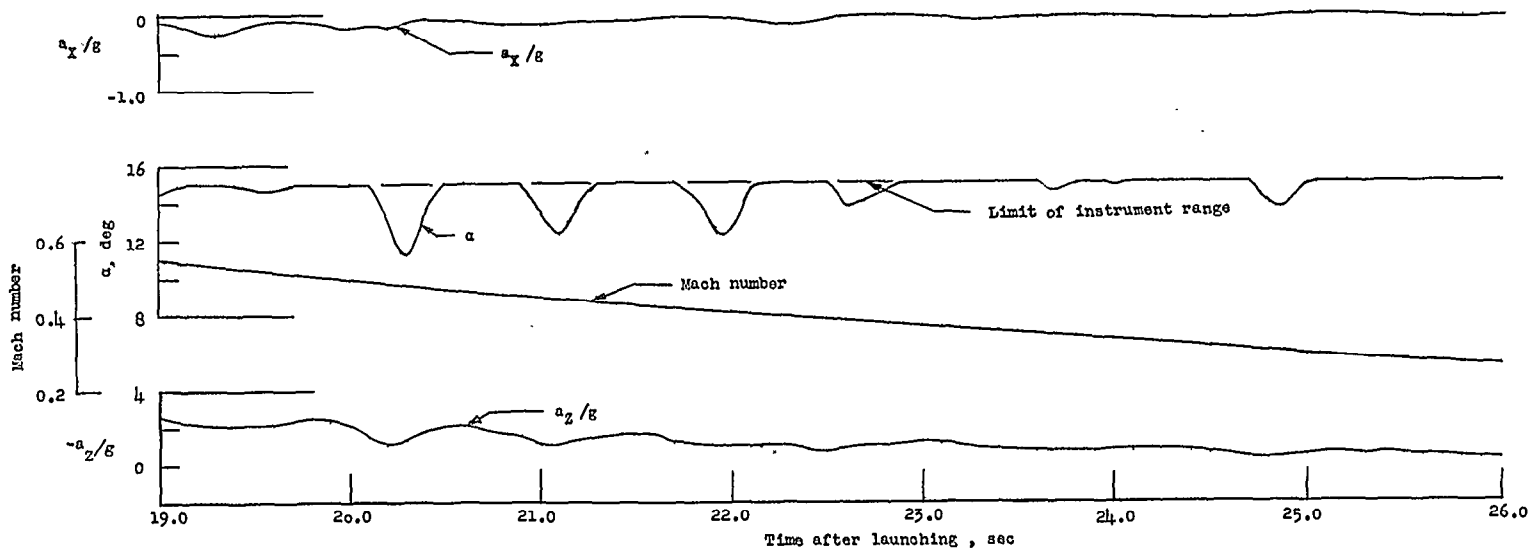


Figure 13.- External drag coefficient as a function of Mach number.



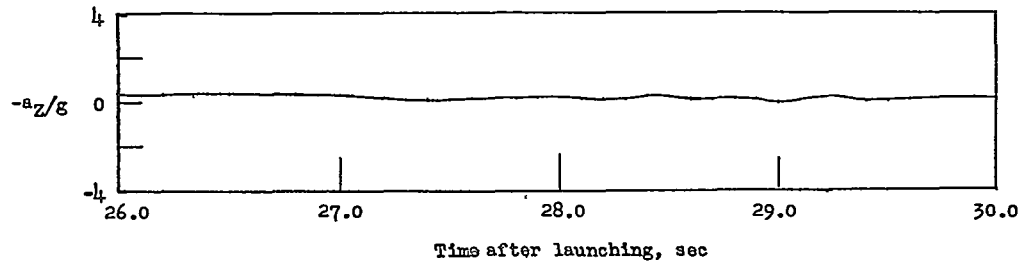
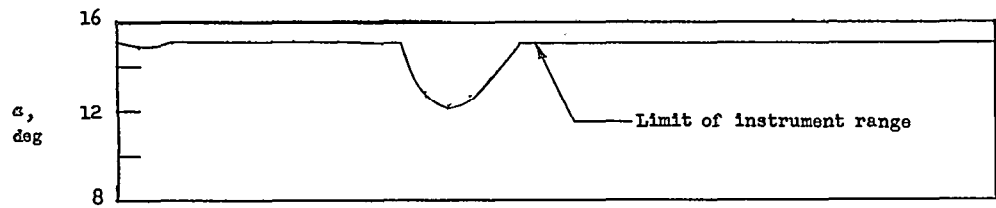
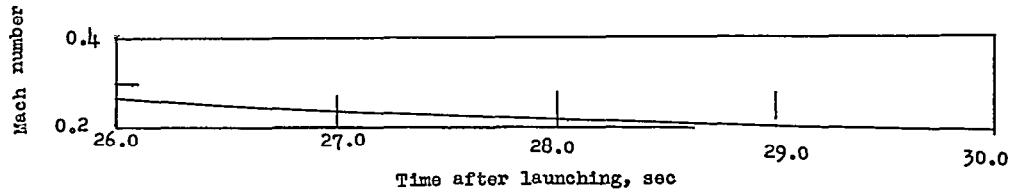
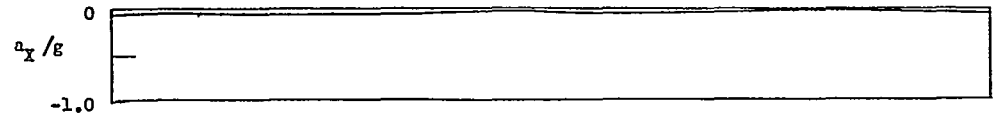
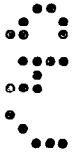
(a)  $M = 1.18$  to  $M = 0.55$ .

Figure 14.- Time histories.



(b)  $M = 0.55$  to  $M = 0.26$ .

Figure 14.- Continued.



(c)  $M = 0.26$  to  $M = 0.19$ .

Figure 14.- Concluded.

100  
100  
100

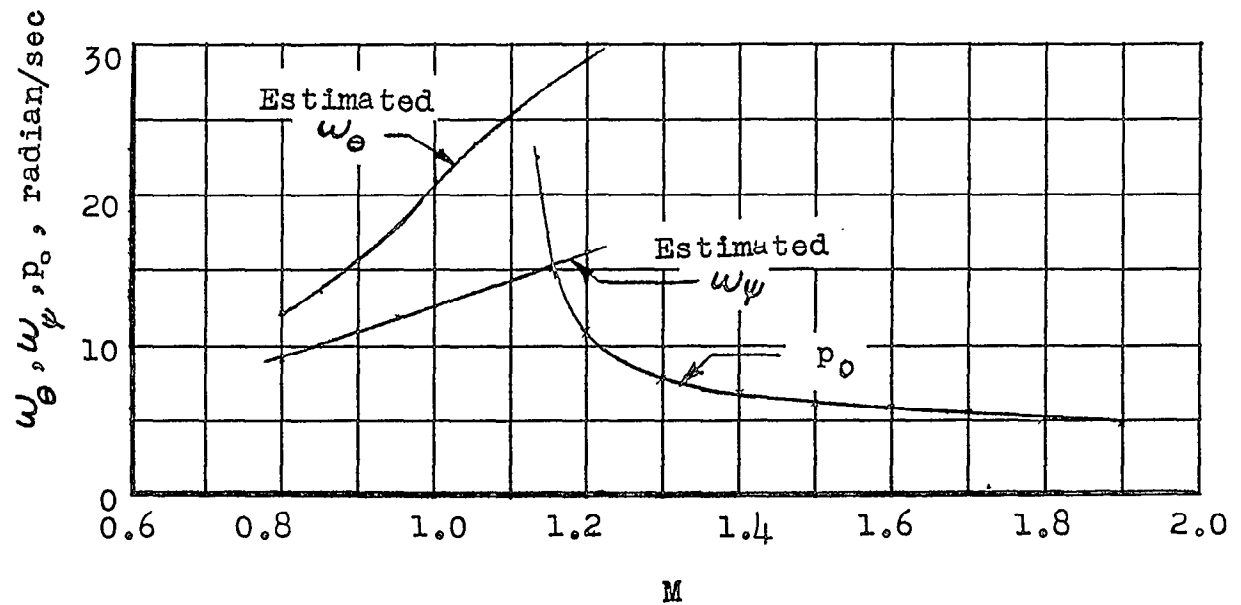


Figure 15.- Model rolling velocity and estimated natural pitch and yaw frequencies.

RESULTS OF THE FLIGHT TEST OF A 0.13-SCALE ROCKET-BOOSTED  
MODEL OF THE McDONNELL F4H-1 AIRPLANE BETWEEN  
MACH NUMBERS OF 0.20 AND 1.90

TEST NO. NACA AD 3115

By Earl C. Hastings, Jr., and Waldo L. Dickens

ABSTRACT

A flight investigation was conducted to determine the low-lift drag of the model at transonic and supersonic speeds; however, at Mach numbers below  $M = 1.17$  the model experienced large pitch oscillations and an analysis of the drag at those Mach numbers was not possible. This paper presents the external drag coefficients between Mach numbers of 1.17 and 1.90 and a qualitative discussion of the pitching oscillations.

INDEX HEADINGS

Airplanes - Specific Types	1.7.1.2
Stability, Longitudinal - Dynamic	1.8.1.2.1

RESULTS OF THE FLIGHT TEST OF A 0.13-SCALE ROCKET-BOOSTED  
MODEL OF THE McDONNELL F4H-1 AIRPLANE BETWEEN  
MACH NUMBERS OF 0.20 AND 1.90

TEC NO. NACA AD 3115

*Earl C. Hastings Jr.*  
Earl C. Hastings, Jr.

*Waldo L. Dickens*  
Waldo L. Dickens

Approved:

*Joseph A. Shortal*  
Joseph A. Shortal  
Chief of Pilotless Aircraft Research Division  
Langley Aeronautical Laboratory

ml  
(10/25/57)



UNCLASSIFIED

~~CONFIDENTIAL~~